water

MDPI

Article

Comparisons of Precipitation Isotopic Effects on Daily, Monthly and Annual Time Scales—A Case Study in the Subtropical Monsoon Region of Eastern China

Zhuoyong Xiao [1], Xinping Zhang [1,2,*], Xiong Xiao [1,2,*], Xin Chang [1], Xinguang He [1,2] and Cicheng Zhang [1]

[1] College of Geographical Sciences, Hunan Normal University, Changsha 410081, China
[2] Key Laboratory of Geospatial Big Data Mining and Applications in Hunan Province, Hunan Normal University, Changsha 410081, China
* Correspondence: zxp@hunnu.edu.cn (X.Z.); xiaoxiong@hunnu.edu.cn (X.X.); Tel.: +86-13308486420 (X.Z.); +86-18813049418 (X.X.)

Abstract: The study on precipitation isotope variation can potentially improve the understanding of weather processes, regional water cycle and paleoclimate reconstruction in the subtropical monsoon region. Based on the measured stable isotope composition in precipitation ($\delta^{18}O_p$) and daily precipitation from January 2010 to December 2021 in Changsha of the subtropical monsoon region of eastern China, the $\delta^{18}O_p$ variations, amount effect and local meteoric water line (LMWL) were analyzed and compared on daily, monthly and annual time scales, as well as under different precipitation intensities. The results showed that, on the daily time scale, $\delta^{18}O_p$ was significantly and negatively correlated with precipitation in the study area. Influenced by subcloud evaporation, small precipitation events ($\leq$5 mm/d) could change the rainout level of precipitation isotopes. There were significant differences in the slope and intercept of the LMWL on different time scales, in different seasons and under different precipitation intensities. On the daily and monthly time scales, the slope and intercept of the LMWL in the cold half of the year were significantly smaller and larger than those in the warm half of the year, respectively, and the slope and intercept of the LMWL increased significantly with precipitation intensity, and then remained largely stable. On the annual time scale, the slope and intercept of the LMWL in the cold half of the year were smaller than those in the warm half of the year. The possible reasons for the differences in the LMWL on different time scales are the combined effects of seasonal differences in precipitation intensity and water vapor sources.

Keywords: Changsha; precipitation; stable isotopes; time scale; rainout

check for updates

Citation: Xiao, Z.; Zhang, X.; Xiao, X.; Chang, X.; He, X.; Zhang, C. Comparisons of Precipitation Isotopic Effects on Daily, Monthly and Annual Time Scales—A Case Study in the Subtropical Monsoon Region of Eastern China. *Water* **2023**, *15*, 438. https://doi.org/10.3390/w15030438

Academic Editor: Cesar Andrade

Received: 21 December 2022
Revised: 12 January 2023
Accepted: 18 January 2023
Published: 22 January 2023

1. Introduction

The heavy isotopes in precipitation (i.e., ^2H and ^{18}O) have stable geophysical–chemical characteristics and respond sensitively to changes in the atmospheric environment. Therefore, the stable isotopic compositions in precipitation (i.e., δ^2H_p and $\delta^{18}O_p$) are often used as quantitative proxies for water cycle tracing, atmospheric circulation pattern diagnosis and paleoclimate reconstruction [1–6].

In many cases, stable isotopes in precipitation show a significant negative correlation with precipitation amount [7]. This phenomenon, called the "amount effect", universally appears in the low-latitude ocean and monsoon regions [8–10]. However, at some mid-latitude stations, the amount effect may occur only in summer [11]. In paleoclimate and hydrometeorological studies, stable isotope compositions in different water bodies have been used as indicators of precipitation intensity or monsoon intensity based on the amount effect [12,13]. According to the Rayleigh fractionation principle [7], the amount effect arises as a result of stable isotope fractionation during condensation. Due to the preferential condensation of heavy isotopes during the phase change, the heavy isotopes in the remaining water vapor are continuously depleted, which leads to the continuous depletion of heavy isotopes in the following precipitation. The higher the cumulative amount of a precipitation event, the stronger the depletion of stable isotopes in water vapor, and the lower the δ^2H_p and $\delta^{18}O_p$. In addition, δ^2H_p and $\delta^{18}O_p$ are also influenced by subcloud evaporation [14–16].

The linear relationship between δ^2H_p and $\delta^{18}O_p$, famous as the meteoric water line (MWL), indicates the average fractionation rate difference among two stable isotopes [7]. On the global scale, MWL was described as $\delta^2H = 8\delta^{18}O + 10‰$ [17]. However, the local MWL (LMWL) varies from place to place and on different time scales [18]. When a water body evaporates in an unsaturated atmosphere, the combined effect of light isotope preferential evaporation and kinetic fractionation effects accelerate the ratio of ^2H to ^{18}O fractionation effects in evaporating water vapor, resulting in an increase in the LMWL slope and deuterium excess (*d*) in water vapor [7,19]. The higher the temperature and the lower the humidity, the higher the LMWL [19]. At the same time, the LMWL slope and *d* decrease in evaporated water bodies, such as raindrops falling from the clouds. In supersaturated environments, the combined action of heavy isotope preferential condensation and kinetic fractionation effects decelerates the ratio between the ^2H and ^{18}O fractionation effects in condensation, leading to a decrease in the LMWL slope and *d* [20]. Additionally, the recycled water vapor from the underlying surface also plays a positive role in the LMWL slope and *d* [20,21]. Generally, the slopes and intercepts of LMWLs are greater in humid regions than in arid regions, and greater in the wet season than in the dry season.

Isotopic effects in precipitation change with time, location and atmospheric circulation conditions [22,23]. Previous studies mainly investigated the stable isotope effects in precipitation based on monthly precipitation data [24–26]. However, limited by the length of the monitoring station data, the following questions require further study: (1) the differences in stable isotopes in precipitation on different time scales; (2) whether the stable isotope effect in precipitation is stable and (3) how stable isotope effects in precipitation vary with precipitation intensity in the monsoon region.

This paper aims to compare the relationship between $\delta^{18}O_p$ and precipitation on daily, monthly and annual time scales, and analyze the LMWL variation on different time scales, based on the 12-year daily δ^2H and $\delta^{18}O$ in precipitation observations in Changsha, and the corresponding daily precipitation from 2010 to 2021. The results will deepen the understanding of stable isotope variation patterns in precipitation in the monsoon region, and provide a basis for regional water cycle research, water resource investigation and paleoclimate reconstruction.

2. Materials and Methods

2.1. Overview of the Study Area

Changsha is located in the eastern subtropical monsoon region of China (Figure 1), with a mild and humid climate and distinct four seasons. The mean annual temperature is 17.4 °C and mean annual precipitation amount is 1447.0 mm. During the warm half of the year (April to September), influenced by the southwest monsoon from the Bay of the Bengal, the Arabian Sea and the southeast monsoon from the western Pacific Ocean, precipitation is abundant and accounts for about 69% of the annual precipitation. During the cold half of the year (October to March), precipitation is low and only accounts for about 31% of the annual precipitation due to continental air masses prevailing.

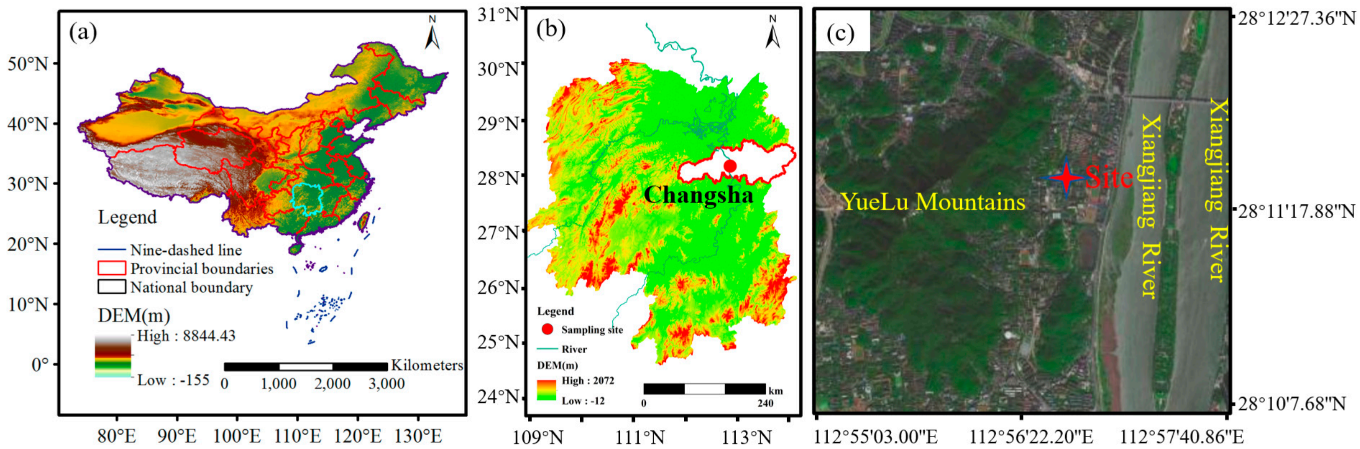

Figure 1. (**a**) Topographic map of China. (**b**) Topographic map of Hunan. (**c**) Locations of sampling sites and weather stations at Hunan Normal University.

2.2. Water Sample Collection

Precipitation sample collection was carried out from 1 January 2010 to 31 December 2021, at the meteorological station of Hunan Normal University, located at the foot of the Yuelu Mountain in Changsha City, China. According to precipitation observation regulation published by the China Meteorological Administration, precipitation of ≥0.1 mm was sampled at 08:00 and at 20:00 (Beijing time) on the rainy day. Precipitation samples were collected by a siphon rain gauge, and the liquid precipitation collected was directly poured into a 30 mL polyethylene plastic bottle and then measured, sealed and numbered. For solid precipitation (snow, hail, etc.), the sample was firstly put into a water sample bag, tightened and placed at room temperature, and then sealed in a 30 mL polyethylene plastic bottle after it completely melted. The water samples were stored at a low temperature (~4 °C) to avoid evaporation.

δ^2H_p and $\delta^{18}O_p$ in water samples were measured using a gas–liquid dual-use water stable isotope analyzer (DLT-IWA-35EP, LGR, USA). Analytical results are expressed as per mill, relative to those of the Vienna Standard Mean Ocean Water (V-SMOW).

$$\delta^{18}\mathrm{O}\ (\text{or}\ \delta^2\mathrm{H}) = (R_\mathrm{s}/R_{\text{v-smow}} - 1) \times 1000‰ \quad (1)$$

where R_s and $R_{\text{v-snow}}$ represent the oxygen (or hydrogen) stable isotope ratios ($^{18}O/^{16}O$ or $^2H/^1H$) in water samples and Vienna Standard Average Ocean Water, respectively. $\delta^{18}O_p$ and δ^2H_p have the precisions of ±0.6‰ and ±0.2‰, respectively.

The data of precipitation and other meteorological elements during the sampling period were obtained from an automatic weather station (WeatherHawk500, Logan, UT, USA) installed at the observation site.

The sampling and monitoring period was 12 natural years. For days including more than one precipitation sample, $\delta^{18}O_p$ and δ^2H_p were calculated using the precipitation-weighted mean. Overall, we obtained 1544 precipitation samples, representing 1544 precipitation days.

3. Results and Discussion

3.1. Temporal Variation in Stable Isotopes in Precipitation

The daily variations in $\delta^{18}O_p$, deuterium excess (d) (d = δ^2H-8δ^{18}O), daily precipitation (P) and mean temperature (T) in Changsha during the study period are shown in Figure 2. According to Figure 2, a unimodal pattern is shown by T variation, ranging from −7.3 to 33.1 °C. The long-term mean T is 15.8 °C, of which 22.3 °C is for the warm half of the year and 9 °C is for the cold half of the year. The variation in daily precipitation also shows a clear unimodal pattern, reaching its peak in a similar period of T. On the daily time scale, the long-term daily mean P is 10.98 mm, of which 14.41 mm is in the warm half of the year and 7.34 mm is in the cold half of the year. The $\delta^{18}O_p$ ranges from −18.1‰ to 5.8‰, and the long-term precipitation-weighted mean $\delta^{18}O_p$ is −6.5‰. It is not consistent with the seasonality of T and P. The long-term precipitation-weighted mean $\delta^{18}O_p$ in the cold half of the year (−5.7‰) is significantly higher than that in the warm half of the year (−7.0‰). The d ranges from −8.9‰ to 33.3‰, with a long-term precipitation-weighted mean value of 14.5‰. Similarly to the seasonal cycle of $\delta^{18}O_p$, the mean d during the cold half of the year (14.5‰) is close to that during the warm half of the year (14.4‰).

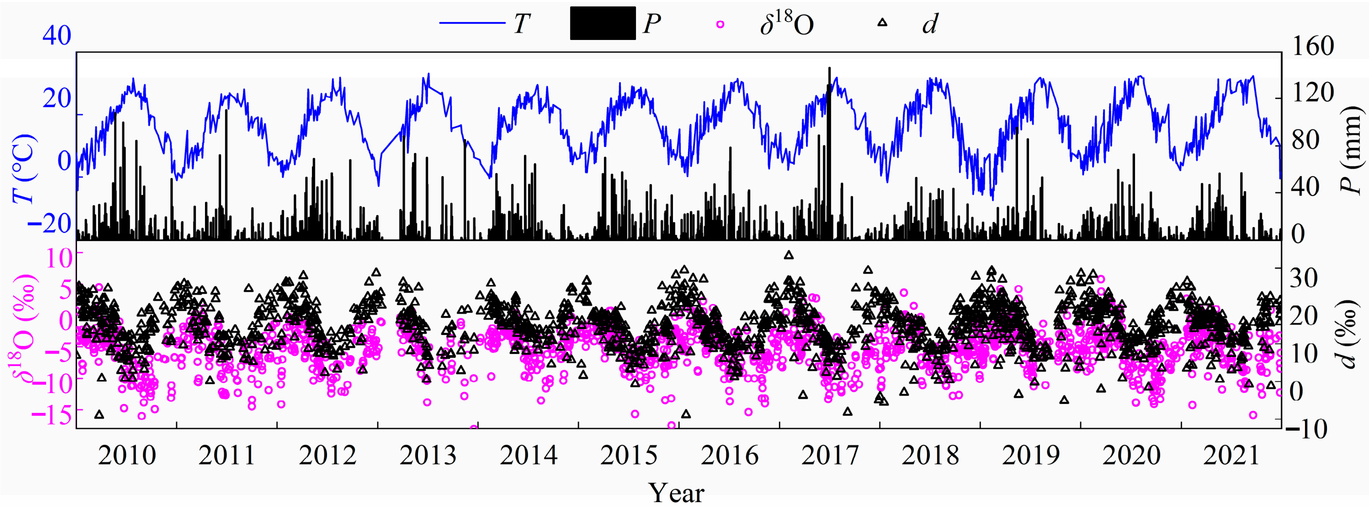

Figure 2. Temporal variation in daily temperature (*T*), precipitation (*P*), $\delta^{18}O_p$ and *d*-excess (*d*), from 1 January 2010 to 31 December 2021, at Changsha station.

The temporal variations in monthly $\delta^{18}O$, *d*, *P* and *T* are shown in Figure 3. the monthly *T* varies from −1.9 to 31.5 °C. In a year, the maximum monthly *T* usually occurs in August, and the minimum is in February. The long-term monthly mean *P* is 118.28 mm, of which 158.56 mm is in the warm half of the year and 77.43 mm is in the cold half of the year. The maximum monthly precipitation usually occurs in June and the minimum occurs in January. The monthly $\delta^{18}O_p$ ranges from −13.1‰ to −1.3‰. The highest monthly $\delta^{18}O_p$ occurs in March and the lowest one occurs in December, which are not consistent with *P* and *T*. The long-term monthly mean *d* ranged from 4.3‰ to 23.0‰ (Jan). The largest and the smallest monthly *d* appeared in January and August, respectively, which are consistent with *T*.

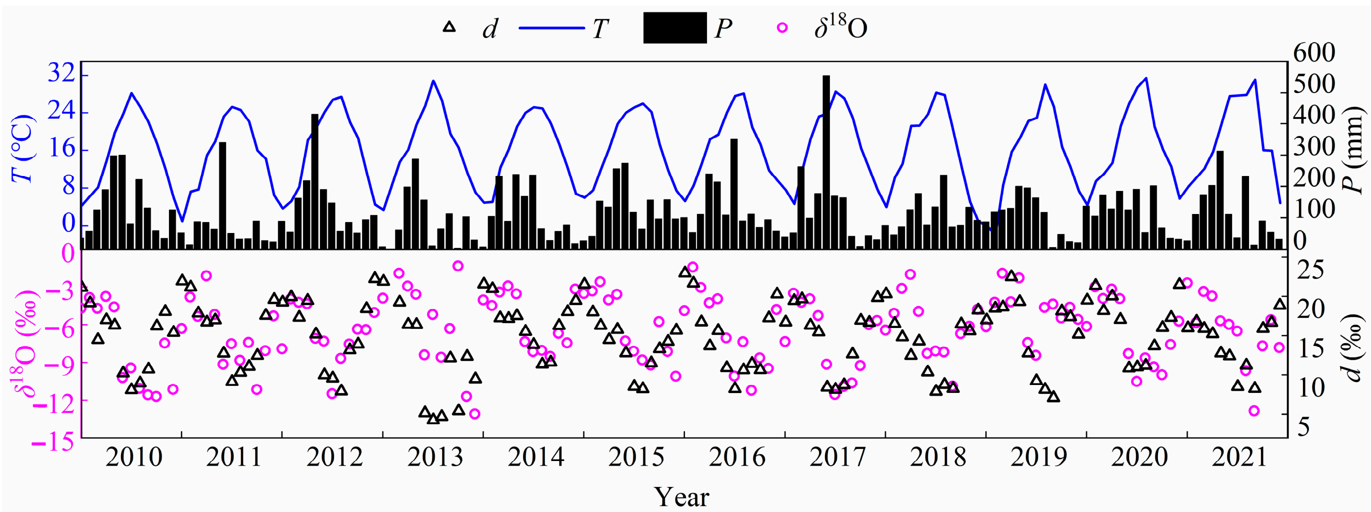

Figure 3. Temporal variations in monthly temperature (*T*), precipitation (*P*), $\delta^{18}O_p$ and *d*-excess (*d*) in Changsha.

On the annual time scale (Figure 4), the mean annual T ranges from 12.3 to 18.9 °C. The maximum mean annual T of 18.9 °C appears in 2013, and the minimum of 12.3 °C appears in 2019. The difference between them is 6.6 °C. The mean annual P ranges from 907 to 1699 mm, with a long-term mean of 1412 mm. The average precipitation in the warm half of the year is 954 mm and that in the cold half of the year is 458 mm. The maximum annual precipitation of 1699 mm occurs in 2012 and the minimum of 907 mm occurs in 2011. The annual $\delta^{18}O_p$ ranges from −7.9‰ to −4.9‰, in which the highest $\delta^{18}O$ occurs in 2019 and the lowest one occurs in 2010 with a difference of 3.1‰ between the two years. The interannual variation in d is consistent with that of $\delta^{18}O$, ranging from 13.0‰ to 16.4‰. The largest annual average d occurs in 2014 and the smallest one occurs in 2013 with a difference of 3.5‰ between the two years. It can be seen that the years with extreme $\delta^{18}O_p$ do not correspond to those with extreme temperature and precipitation.

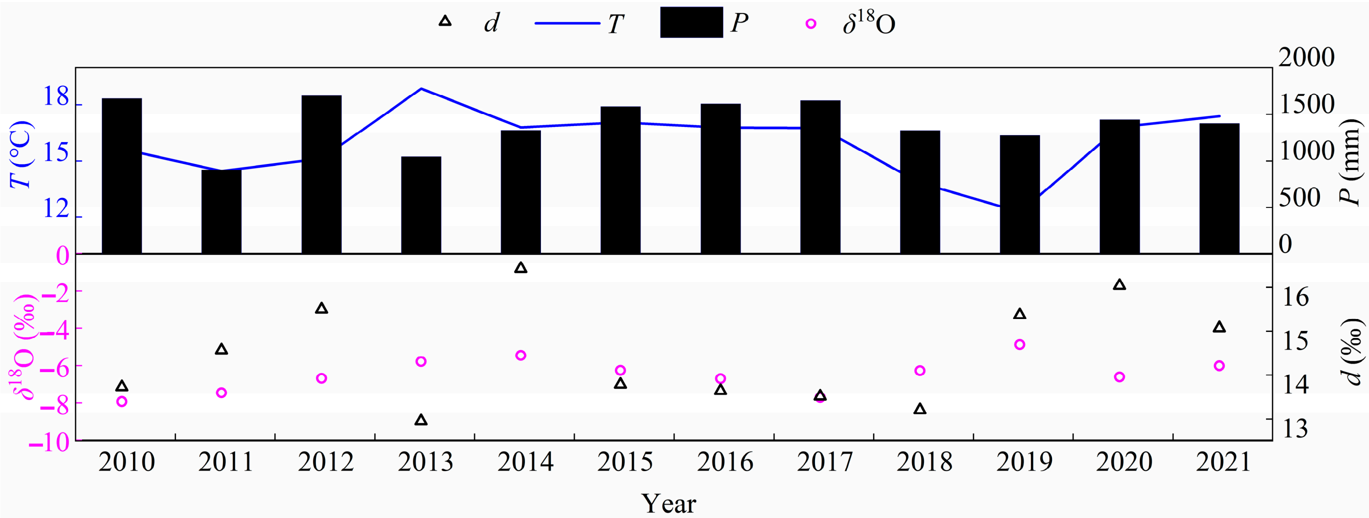

Figure 4. Temporal variations in annual temperature (T), precipitation (P), $\delta^{18}O_p$ and d-excess (d) in Changsha.

Although stable isotopes in precipitation or temperature have the same weighted mean or mean value on daily, monthly and annual time scales, there are significant differences in their dispersion levels. For example, the standard deviations of the weighted mean $\delta^{18}O$ are 3.4‰, 2.7‰ and 0.9‰ on the three time scales; 5.9‰, 4.4‰ and 1.1‰ for the weighted mean d; and 8.7 °C, 8.2 °C and 1.7 °C for the mean temperature, respectively. This indicates that the variation range of each element varies on different time scales. Since the precipitation is cumulative, the average precipitation amounts on the three time scales are 11mm (mean daily), 118mm (mean monthly) and 1412mm (mean annual), respectively, and their standard deviations are 15.37mm, 89.83mm and 240.74mm, respectively.

3.2. Relationship between $\delta^{18}O_p$ and Precipitation Amount

In paleoclimate and hydrometeorological studies, stable isotope compositions in precipitation are often considered as proxies for humidity or monsoon intensity [12,13], especially in low-latitude marine and monsoon regions. Usually, the intensity of the amount effect is mainly dependent on the slope of the $\delta^{18}O_p$-P linear regression. It represents the rainout level of $\delta^{18}O_p$ during the phase change [7].

To reveal the seasonal differences in amount effect and the variation in amount effect with precipitation intensity in the study area, scatter plots of $\delta^{18}O_p$ versus P on three different time scales (daily, monthly and annual) and in three different periods (annual, warm half of the year and cold half of the year) are shown in Figure 5. By calculating the $\delta^{18}O_p$-P correlations for daily precipitation of ≥5.0 mm, 10.0 mm and 25.0 mm, Table 1 is obtained. In order to make the statistical results more reasonable, the sample size in each group should be more than 12.

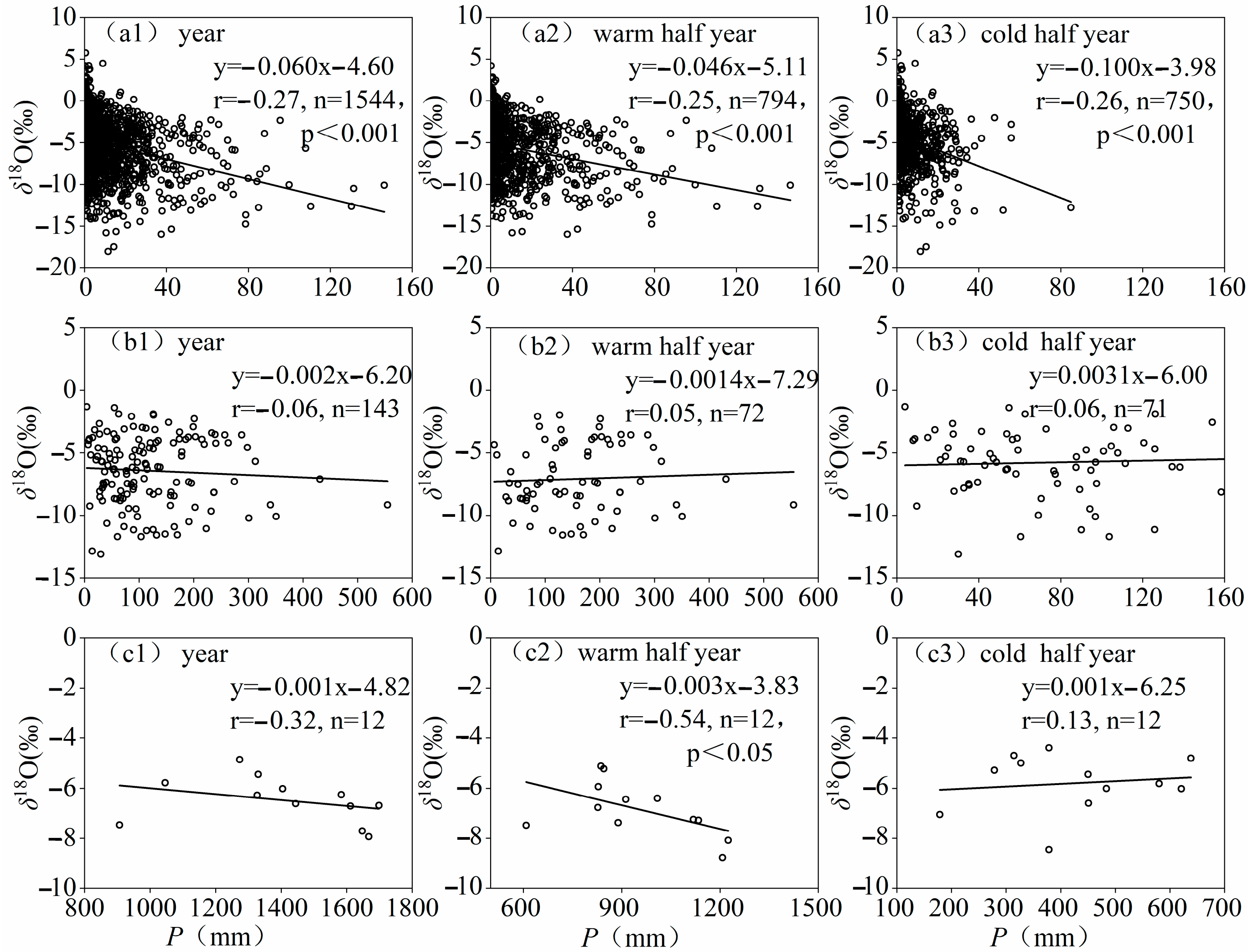

Figure 5. Correlated scatters of $\delta^{18}O_p$ versus precipitation (P) in Changsha on daily (**a1**,**a2**,**a3**), monthly (**b1**,**b2**,**b3**) and annual (**c1**,**c2**,**c3**) time scales in three periods: entire year (**a1**,**b1**,**c1**), warm half of the year (**a2**,**b2**,**c2**) and cold half of the year (**a3**,**b3**,**c3**) ($p > 0.05$ is not marked in the figure).

On the daily time scale (Figure 5a), a significant negative correlation between $\delta^{18}O_p$ and daily P is observed for all three time periods. All correlation coefficients reach the significance level of 0.001, indicating that the amount effect exists in the study area. In comparison, the slope of −0.10‰/mm and the intercept of −3.92‰ for δ^{18}O-P in the cold half of the year are larger than those in the warm half of the year (−0.046‰/mm and −5.04‰), indicating that the rainout level is relatively higher in the cold half of the year than in the warm half of the year.

In addition to seasonal differences, the amount effect also varies with precipitation intensity. As can be seen from Table 1, when the daily precipitation intensity increases from >0.0 mm to ≥5.0 mm, the δ^{18}O-P slope decreases significantly and the intercept increases significantly for all three time periods. With the increase in daily precipitation intensity, both the δ^{18}O-P slope and the intercept do not change much. This result suggests that small precipitation events below 5.0 mm/d can change the rainout level of precipitation isotopes. It has been pointed out that the evaporative enrichment of stable isotope composition in raindrops occurs mainly during small precipitation events [16]. The result of evaporative enrichment of stable isotopes in raindrops causes an upward shift of the left end of the δ^{18}O-P regression line, which leads to an increase in the slope of the regression line and a decrease in the intercept.

Table 1. Correlations of δ^{18}O in precipitation versus precipitation under different precipitation intensities on daily and monthly time scales in Changsha.

Time Scale	Time Interval	$p > 0.0$ mm	≥5.0 mm	≥10.0 mm	≥25.0 mm	≥50.0 mm
Daily	Year	−0.0596/−4.60 −0.27 †	−0.0419/−5.23 −0.23 †	−0.0367/−5.46 −0.21 †	−0.0379/−5.45 −0.25 †	−0.0437/−4.85 −0.29 *
	Warm half of the year	−0.0462/−5.11 −0.25 †	−0.0361/−5.55 −0.23 †	−0.0307/−5.82 −0.20 †	−0.0379/−5.44 −0.26 ‡	−0.0416/−4.94 −0.29 *
	Cold half of the year	−0.0961/−3.98 −0.27 †	−0.0532/−4.82 −0.16 ‡	−0.0545/−4.81 −0.16 *	−0.0443/−5.30 −0.15	−0.1580/1.520 −0.45
		$p > 0.0$ mm	**≥50.0 mm**	**≥100.0 mm**	**≥150.0 mm**	**≥200.0 mm**
Monthly	Year	−0.0019/−6.20 −0.06	−0.0013/−6.29 −0.04	−0.0042/−5.57 −0.12	−0.0054/−5.20 −0.15	−0.0116/−3.17 −0.34
	Warm half of the year	0.0014/−7.29 0.05	−0.0001/−6.93 −0.00	−0.0022/−6.42 −0.07	−0.0031/−6.14 −0.09	−0.0106/−3.66 −0.32
	Cold half of the year	0.0031/−6.01 0.06	0.0115/−7.05 0.19	0.0137/−7.04 0.23	0.0076/−5.68 0.18	

Note: The first row is the slope/intercept and the second row is the correlation coefficient; the symbols *, ‡ and † indicate the correlation coefficient exceeding the confidence levels of 0.05, 0.01 and 0.001, respectively.

On the monthly time scale (Figure 5b), there is no significant negative correlation between monthly $\delta^{18}O_p$ and monthly P for all three time periods. However, according to Table 1, a negative correlation between the monthly weighted average δ^{18}O and monthly P exists to some extent only during the annual period and only when monthly precipitation is greater than or equal to 200 mm, with the correlation coefficients reaching the 0.1 significance level. In the study area, monthly precipitation exceeding 200 mm occurs mainly during the rainy season in the warm half of the year. Therefore, it can be concluded that there is a significant amount effect during the rainy season in the warm half of the year in the study area. The slope of δ^{18}O-P on the monthly time scale is significantly smaller than that on the daily time scale.

On the annual time scale (Figure 5c), there is a very weak negative correlation between the annual $\delta^{18}O_p$ and annual P. During the warm half of the year, the negative correlation between $\delta^{18}O_p$ and P reaches a confidence level of 0.05. In the cold half of the year, there is an insignificant positive correlation between the annual $\delta^{18}O_p$ and the annual P.

3.3. Comparison of Meteoric Water Lines

The regression equation between δ^2H and δ^{18}O in atmospheric precipitation is called the meteoric water line (MWL), which is divided into the global meteoric water line GMWL and the local meteoric water line LMWL [17]. The difference between them both is mainly reflected in the difference in spatial scales. We take the GMWL as the average. Then, are there also significant differences in meteoric water lines on different time scales and under different precipitation intensities?

In order to answer the above question, Figure 6 shows the scatters between δ^2H and δ^{18}O in precipitation on three different time scales (daily, monthly and annual) and in three different periods (annual, warm half of the year and cold half of the year) in the study area. In addition, the variations in local meteoric water lines (LMWLs) with precipitation intensities on daily and monthly time scales are shown in Table 2.

On the daily time scale (Figure 6a), the slope of the LMWL in the cold half of the year (7.99) is significantly smaller than that in the warm half of the year (8.32), but its intercept (17.58) is larger than that in the warm half of the year (14.04), indicating that the vapor source of generating precipitation varies with seasons [27,28]. The slope and intercept of the LMWL in the annual period intermediate between the two halves of the year. Usually, the slope of the LMWL is proportional to the intercept [9], but in the monsoon region, the $\delta^{18}O_p$ and δ^2H_p in the cold half of the year are higher than those in the warm half of the year, which leads to the scatters in the cold half of the year being in the upper right of the

δ^2H-δ^{18}O diagram compared with those in the warm half of the year, resulting in a larger intercept of the LMWL in the cold half of the year than in the warm half of the year.

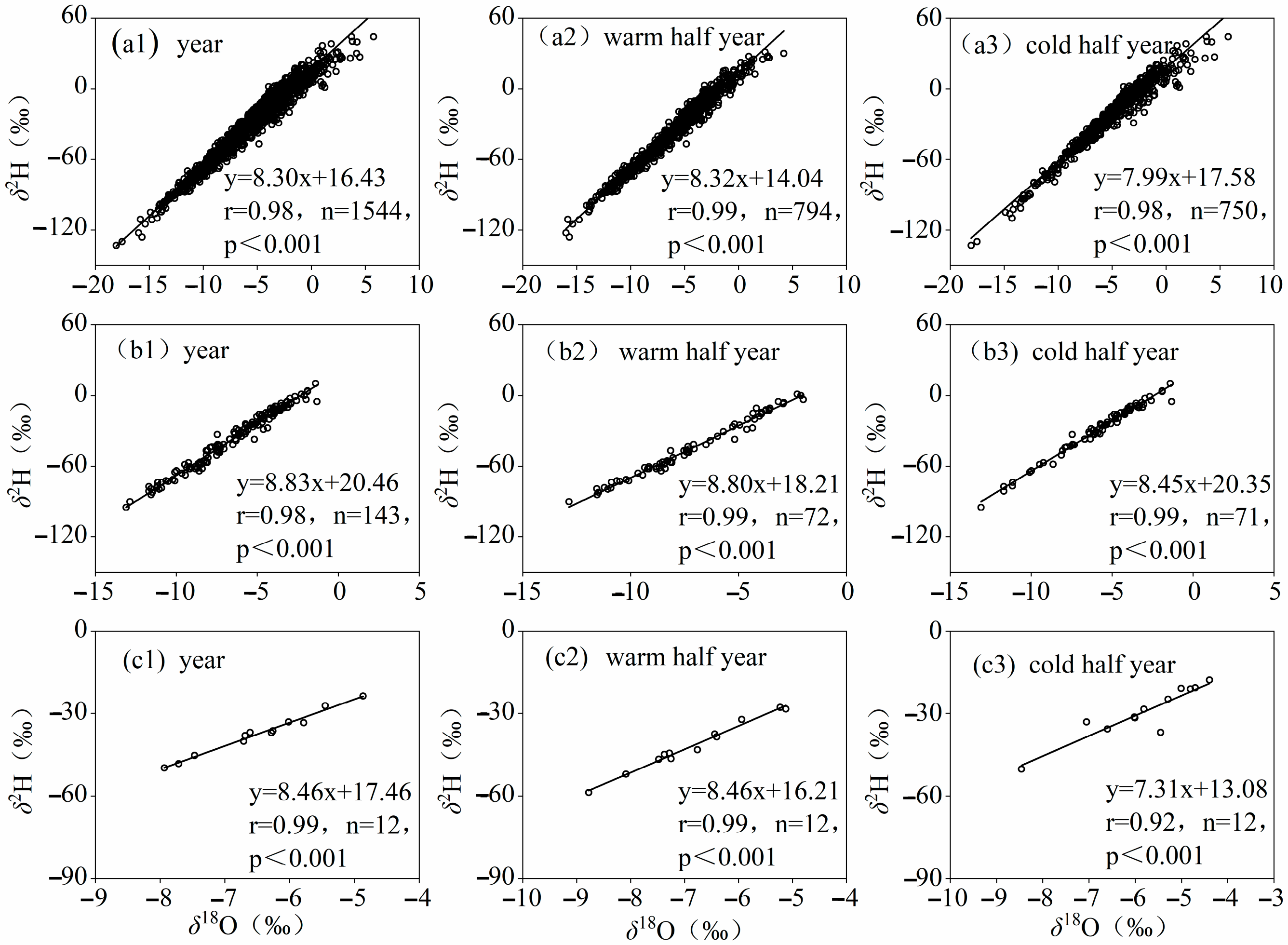

Figure 6. Variations in LMWLs on daily (**a1**,**a2**,**a3**), monthly (**b1**,**b2**,**b3**) and annual (**c1**,**c2**,**c3**) time scales in three periods: entire year (**a1**,**b1**,**c1**), warm half of the year (**a2**,**b2**,**c2**) and cold half of the year (**a3**,**b3**,**c3**) in Changsha.

Table 2. Variations in the local meteoric water lines (LMWLs) with precipitation intensities on daily and monthly time scales in Changsha (slope/intercept).

Time Scale	Time Interval	p > 0.0 mm	≥5.0 mm	≥10.0 mm	≥25.0 mm	≥50.0 mm
Daily	Year	8.30/16.43	8.59/18.81	8.64/18.56	8.71/18.92	8.69/18.35
	Cold half of the year	8.32/14.04	8.60/17.11	8.62/17.44	8.72/18.50	8.70/18.20
	Warm half of the year	7.99/17.58	8.37/19.92	8.47/20.23	8.59/20.34	8.71/20.47
		p > 0.0 mm	**≥50.0 mm**	**≥100.0 mm**	**≥150.0 mm**	**≥200.0 mm**
Monthly	Year	8.83/20.46	8.91/20.72	8.96/20.57	9.06/20.88	9.03/21.12
	Cold half of the year	8.81/18.21	8.96/19.52	8.91/19.46	9.06/20.70	8.99/20.75
	Warm half of the year	8.45/20.35	8.52/20.52	8.54/20.42	8.49/19.13	

Different precipitation intensities have different condensation conditions in the cloud and different environmental conditions under the cloud, and thus directly affect the fractionation effect of ^{2}H and ^{18}O, and change the LMWL. As can be seen from Table 2, the slope and intercept of the LMWL increase significantly with the increase in precipitation intensity from ≥0.0 mm to ≥5.0mm in the three periods. After that, both the slope and the intercept of the LMWL remain almost unchangeable with the increase in daily precipitation intensity. This result suggests that small precipitation events below 5.0 mm/d can significantly change local meteoric water lines. It has been demonstrated [16] that the evaporation enrichment of stable isotopes in falling raindrops during small precipitation events will lead to a decrease in the slope and intercept of the LMWL.

On the monthly time scale (Figure 6b), the slope of the LMWL in the cold half of the year (8.45, with a standard error of 0.14) is smaller than that in the warm half of the year (8.80, with a standard error of 0.14), but its intercept (20.35) is obviously larger than that in the warm half of the year (18.21), also reflecting the seasonal differences in vapor sources that generate precipitation. Compared with the LMWL on the daily time scale, the slope and intercept of the LMWL on the monthly time scale for all three time periods are significantly larger, and increase with monthly precipitation intensity, especially with regard to the low precipitation intensity. This is related to the seasonal variation characteristics of stable isotopes in precipitation, and also to the application of the precipitation-weighted mean algorithm. In the East Asian monsoon region, strong precipitation usually corresponds to low isotopic values [28–32]. Owing to the applied precipitation-weighted mean algorithm, the precipitation samples at the upper right end of the δ^2H-δ^{18}O scatter plot will shift to the left relative to the lower left end, and this will result in an increase in the slope and intercepts of the LMWL on monthly time scales.

On the annual time scale (Figure 6c), the slope and intercept of the LMWL in the cold half of the year are smaller than those in the warm half of the year and annual periods. Since the annual statistics have eliminated the continuous seasonal variation and only 12 samples are available for each data set, their reasonableness needs to be tested.

4. Conclusions

Based on the measured stable isotopes in precipitation and the corresponding daily precipitation at Changsha station from 1 January 2010 to 31 December 2021, the temporal variations in stable isotopes in precipitation, amount effect and LMWLs were analyzed and compared on daily, monthly and annual time scales, as well as under different precipitation intensities. The principal results are as follows:

(1) The daily variation in $\delta^{18}O_p$ ranges from −18.1‰ to 5.8‰ in Changsha, the monthly $\delta^{18}O_p$ ranges from −13.1‰ to −1.3‰ and the annual range of $\delta^{18}O_p$ ranges from −7.9‰ to −4.9‰. Overall, the long-term precipitation-weighted mean $\delta^{18}O_p$ in the cold half of the year (−5.7‰, with a standard error of 3.4) is significantly higher than that in the warm half of the year (−7.0‰, with a standard error of 3.4).

(2) On the daily time scale, a significant negative correlation between $\delta^{18}O_p$ and daily P is observed for all three time periods, indicating the amount effect that exists in the study area. In comparison, the rainout level is relatively higher in the cold half of the year than in the warm half of the year, and the amount effect also varies with precipitation intensity. This result suggests that small precipitation events below 5.0 mm/d can change the rainout level of precipitation isotopes. There is an insignificant correlation between $\delta^{18}O_p$ and P on both monthly and annual time scales.

(3) There are significant differences in the LMWL corresponding to different time scales, different seasons and different precipitation intensities. On the daily and monthly time scales, the slope and intercept of the LMWL in the cold half of the year are smaller than those of the LMWL in the warm half of the year and in the annual period. However, the slope and intercept of the LMWL remain almost unchangeable with the increasing precipitation intensity afterward. On the annual time scale, the slope and intercept of the LMWL in the cold half of the year are smaller than those in the warm half of the year.

Author Contributions: Conceptualization, Z.X., X.Z., X.X. and X.C.; methodology, Z.X., X.Z., X.H. and X.C.; software, X.H.; validation, Z.X. and X.Z.; formal analysis, Z.X., X.Z., X.X. and X.C.; investigation, Z.X., X.Z., X.X. and X.C.; resources, X.Z.; data curation, X.Z.; writing—original draft preparation, Z.X., X.Z., X.X. and X.C.; writing—review and editing, Z.X., X.Z., X.X., C.Z. and X.C.; visualization, Z.X. and X.Z.; supervision, X.Z., X.X., X.H. and C.Z.; project administration, X.Z. and X.X.; funding acquisition, X.Z. and X.X. All authors have read and agreed to the published version of the manuscript.

Funding: This research was funded by the National Natural Science Foundation of China (Grant number 42101130).

Data Availability Statement: The data that support the findings of this study are available from the corresponding author upon reasonable request.

Conflicts of Interest: The authors declare that they have no known competing financial interests or personal relationships that could have appeared to influence the work reported in this paper.

References

1. Wu, H.; Li, X.Y.; Zhang, J.; Li, J.; Liu, J.; Tian, L.; Fu, C. Stable isotopes of atmospheric water vapour and precipitation in the northeast Qinghai-Tibetan Plateau. *Hydrol. Process.* **2019**, *33*, 2997–3009. [CrossRef]
2. Wu, H.; Huang, Q.; Fu, C.; Song, F.; Liu, J.; Li, J. Stable isotope signatures of river and lake water from Poyang Lake, China: Implications for river–lake interactions. *J. Hydrol.* **2021**, *592*, 125619. [CrossRef]
3. Zhang, X.P.; Liu, J.M.; Wang, X.Y.; Nakawo, M.; Xie, Z.C.; Zhang, J.M.; Zhang, X.Z. Climatological significance of stable isotopes in precipitation over south-west China. *Int. J. Climatol.* **2010**, *30*, 2229–2239. [CrossRef]
4. Laonamsai, J.; Ichiyanagi, K.; Kamdee, K.; Putthividhya, A.; Tanoue, M. Spatial and temporal distributions of stable isotopes in precipitation over Thailand. *Hydrol. Process.* **2021**, *35*, e13995. [CrossRef]
5. Mosley-Thompson, E.; Thompson, L.G.; Grootes, P.M.; Gundestrup, N. Little ice age (neoglacial) paleoenvironmental conditions at siple station, Antarctica. *Ann. Glaciol.* **1990**, *14*, 199–204. [CrossRef]
6. Tan, M. Circulation effect: Response of precipitation δ^{18}O to the ENSO cycle in monsoon regions of China. *Clim. Dyn.* **2014**, *42*, 1067–1077. [CrossRef]
7. Dansgaard, W. Stable isotopes in precipitation. *Tellus* **1964**, *16*, 436–468. [CrossRef]
8. Tian, L.D.; Yao, T.D.; Schuster, P.F.; White, J.W.C.; Ichiyanagi, K.; Pendall, E.; Pu, J.; Yu, W. Oxygen-18 concentrations in recent precipitation and ice cores on the Tibetan Plateau. *J. Geophys. Res. Atmos.* **2003**, *108*. [CrossRef]
9. Yao, T.; Masson-Delmotte, V.; Gao, J.; Yu, W.; Yang, X.; Risi, C.; Sturm, C.; Werner, M.; Zhao, H.; He, Y.; et al. A review of climatic controls on δ^{18}O in precipitation over the Tibetan Plateau: Observations and simulations. *Rev. Geophys.* **2013**, *51*, 525–548. [CrossRef]
10. Kong, Y.; Wang, K.; Li, J.; Pang, Z. Stable isotopes of precipitation in China: A consideration of moisture sources. *Water* **2019**, *11*, 1239. [CrossRef]
11. Moore, M.; Kuang, Z.; Blossey, P.N. A moisture budget perspective of the amount effect. *Geophys. Res. Lett.* **2014**, *41*, 1329–1335. [CrossRef]
12. Fritz, P.; Ch, F.J. Isotopes in cloud physics: Multiphase and multistage condensation process. In *Handbook of Environmental Isotope Geochemistry. Volume 2, the Terrestrial Environment*; Elsevier: New York, NY, USA, 1986; pp. 71–73.
13. Araguás-Araguás, L.; Froehlich, K.; Rozanski, K. Stable isotope composition of precipitation over southeast Asia. *J. Geophys. Res. Atmos.* **1998**, *103*, 28721–28742. [CrossRef]
14. Risi, C.; Bony, S.; Vimeux, F.; Chong, M.; Descroix, L. Evolution of the stable water isotopic composition of the rain sampled along Sahelian squall lines. *Q. J. R. Meteorol. Soc.* **2010**, *136*, 227–242. [CrossRef]
15. Liu, Z.; Tian, L.; Yao, T.; Yu, W. Seasonal deuterium excess in Nagqu precipitation: Influence of moisture transport and recycling in the middle of Tibetan Plateau. *Environ. Geol.* **2008**, *55*, 1501–1506. [CrossRef]
16. Chen, F.; Chen, J.; Wang, S.; Wu, X.; Zhang, Q.; Gao, M.; Kang, X.; Pu, Z.; Zhang, D. Below-cloud evaporation effect on stable water isotopes in precipitation at the eastern margin of Qinghai-Tibet Plateau. *Hydrol. Process.* **2022**, *36*, e14699. [CrossRef]
17. Craig, H. Isotopic variations in meteoric waters. *Science* **1961**, *133*, 1702–1703. [CrossRef]
18. Wang, S.; Zhang, M.; Hughes, C.E.; Crawford, J.; Wang, G.; Chen, F.; Du, M.; Qiu, X. Meteoric water lines in arid Central Asia using event-based and monthly data. *J. Hydrol.* **2018**, *562*, 435–445. [CrossRef]
19. Zhang, X.P.; Liu, J.M.; Nakawo, M.; Xie, Z.C. Vapor origins revealed by deuterium excess in precipitation in southwest China. *J. Glaciol. Geocryol.* **2009**, *31*, 613–619.
20. Zhang, X.P.; Yang, Z.L.; Niu, G.Y.; Wang, X.Y. Stable water isotope simulation in different reservoirs of Manaus, Brazil, by Community Land Model incorporating stable isotopic effect. *Int. J. Climatol. A J. R. Meteorol. Soc.* **2009**, *29*, 619–628. [CrossRef]
21. Cai, Z.; Tian, L. Atmospheric controls on seasonal and interannual variations in the precipitation isotope in the East Asian monsoon region. *J. Clim.* **2016**, *29*, 1339–1352. [CrossRef]
22. Yu, W.; Wei, F.; Ma, Y.; Liu, W.; Zhang, Y.; Luo, L.; Tian, L.; Xu, B.; Qu, D. Stable isotope variations in precipitation over Deqin on the southeastern margin of the Tibetan Plateau during different seasons related to various meteorological factors and moisture sources. *Atmos. Res.* **2016**, *170*, 123–130. [CrossRef]
23. Guo, X.; Gong, X.; Shi, J.; Guo, J.; Domínguez-Villar, D.; Lin, Y.; Wang, H.; Yuan, D. Temporal variations and evaporation control effect of the stable isotope composition of precipitation in the subtropical monsoon climate region, Southwest China. *J. Hydrol.* **2021**, *599*, 126278. [CrossRef]
24. Liu, J.; Song, X.; Yuan, G.; Sun, X.; Yang, L. Stable isotopic compositions of precipitation in China. *Tellus B Chem. Phys. Meteorol.* **2014**, *66*, 22567. [CrossRef]

25. Wu, J.; Ding, Y.; Ye, B.; Yang, Q.; Zhang, X.; Wang, J. Spatio-temporal variation of stable isotopes in precipitation in the Heihe River Basin, Northwestern China. *Environ. Earth Sci.* **2010**, *61*, 1123–1134. [CrossRef]
26. Pang, H.; He, Y.; Lu, A.; Zhao, J.; Ning, B.; Yuan, L.; Song, B. Synoptic-scale variation of δ^{18}O in summer monsoon rainfall at Lijiang, China. *Chin. Sci. Bull.* **2006**, *51*, 2897–2904. [CrossRef]
27. Wu, H.; Zhang, X.; Xiaoyan, L.; Li, G.; Huang, Y. Seasonal variations of deuterium and oxygen-18 isotopes and their response to moisture source for precipitation events in the subtropical monsoon region. *Hydrol. Process.* **2015**, *29*, 90–102. [CrossRef]
28. Li, G.; Zhang, X.; Xu, Y.; Wang, Y.; Wu, H. Synoptic time-series surveys of precipitation δ^{18}O and its relationship with moisture sources in Yunnan, southwest China. *Quat. Int.* **2017**, *440*, 40–51. [CrossRef]
29. Zhou, H.; Zhang, X.; Yao, T.; Hua, M.; Wang, X.; Rao, Z.; He, X. Variation of δ^{18}O in precipitation and its response to upstream atmospheric convection and rainout: A case study of Changsha station, south-central China. *Sci. Total Environ.* **2019**, *659*, 1199–1208. [CrossRef]
30. Benettin, P.; Volkmann, T.H.; von Freyberg, J.; Frentress, J.; Penna, D.; Dawson, T.E.; Kirchner, J.W. Effects of climatic seasonality on the isotopic composition of evaporating soil waters. *Hydrol. Earth Syst. Sci.* **2018**, *22*, 2881–2890. [CrossRef]
31. Tappa, D.J.; Kohn, M.J.; McNamara, J.P.; Benner, S.G.; Flores, A.N. Isotopic composition of precipitation in a topographically steep, seasonally snow-dominated watershed and implications of variations from the Global Meteoric Water Line. *Hydrol. Process.* **2016**, *30*, 4582–4592. [CrossRef]
32. Fritz, M.; Wetterich, S.; McAlister, J.; Meyer, H. A new local meteoric water line for Inuvik (NT, Canada). *Earth Syst. Sci. Data* **2022**, *14*, 57–63. [CrossRef]